



# Structure evolution and microwave absorption properties of nickel nanoparticles incorporated carbon spheres



Zhibin Su\*, Jin Tao, Jianyong Xiang, Yu Zhang, Can Su, Fusheng Wen\*

State Key Laboratory of Metastable Materials Science and Technology, Yanshan University, Qinghuangdao 066004, People's Republic of China

## ARTICLE INFO

### Article history:

Received 5 April 2016

Received in revised form 3 August 2016

Accepted 23 August 2016

Available online 24 August 2016

### Keywords:

- A. Nanostructures
- B. Chemical synthesis
- C. Electron microscopy
- C. X-ray diffraction
- D. Dielectric properties

## ABSTRACT

Carbon spheres were obtained by hydrothermal synthesis using glucose as carbon source, and then nickel nanoparticles were incorporated on carbon spheres by reducing with hydrogen. The nickel nanoparticles (about 6 nm) with magnetic loss were uniformly dispersed on the surface of carbon spheres (200–400 nm) with dielectric loss. The few-layer graphene have been obtained on the carbon spheres by nickel catalysis. The minimum reflection loss value of  $-20.3$  dB was observed at 14.4 GHz with a matching thickness of 9.0 mm for 40 wt.% composites. The nickel nanoparticles incorporated carbon spheres are a promising candidate for excellent microwave absorption materials.

© 2016 Elsevier Ltd. All rights reserved.

## 1. Introduction

Microwave absorbing materials received extensive attention in the civil fields owing to rapid developments of electronic and communication devices [1]. The composites consisted of magnetic metal materials and carbon materials as microwave absorber have been widely studied [2]. Fe [3], Co [4], Ni [5–8], FeCo [9] and FeNi [10], etc. have been proven to be used as excellent microwave absorber with magnetic loss. Graphene [11], carbon nanotubes [12], carbon spheres [13], and fullerene [14], etc. have been comprehensively researched as microwave absorbing materials with dielectric loss. Excellent microwave absorption properties can be achieved by combining magnetic and dielectric loss.

Among above carbon materials, carbon spheres as dielectric loss materials are less studied [13,15]. Moreover, carbon spheres prepared by glucose possess amorphous carbon structure [16]. Metal nickel catalyst can induce few-layer graphene from solid carbon sources [17]. Nickel catalyzed carbon sphere inducing few-layer graphene and corresponding microwave absorption properties have not been reported. In this work, carbon spheres were prepared by glucose using hydrothermal reaction, and nickel nanoparticles incorporated carbon spheres were fabricated by reducing with hydrogen. The nickel nanoparticles incorporated carbon spheres accompanied by few-layer graphene have been

obtained and the corresponding excellent microwave absorption properties have been characterized.

## 2. Experimental

The nickel nanoparticles incorporated carbon spheres were prepared as shown in Fig. 1(a). Carbon spheres with size of around 200–400 nm were prepared following literature methods with some modifications [16]. 0.5 M glucose aqueous solution was transferred into a Teflon-lined stainless steel autoclave and maintained at 190 °C for 1 h. The dark brown suspension was filtered and washed with deionized water and absolute ethyl alcohol. The collected solid sample was dried at 60 °C in oven for overnight. The carbon spheres were dispersed in  $\text{Ni}(\text{NO}_3)_2 \cdot 6\text{H}_2\text{O}$  solution with stirring at 50 °C in a water bath for 5 h. The collected solid sample was centrifuged and dried. The resulting materials were reduced using  $\text{H}_2$  at 500 °C.

The crystal structure of nickel nanoparticles incorporated carbon spheres was examined using x-ray diffraction (XRD) with  $\text{Cu } K\alpha$  radiation on D/MAX-2500 diffractometer. Raman spectra were measured in a Reinshaw inVia microRaman spectroscopy with a laser radiation of 514 nm. The morphology was taken by a scanning electron microscope (S-4800) and transmission electron microscopy (JEOL JEM-2010). The composites for high-frequency magnetic properties measurement were prepared by epoxy resin with 40 wt.% nickel nanoparticles incorporated carbon spheres, and were pressed into toroidal shape ( $\varphi_{\text{out}}$ : 7.00 mm,  $\varphi_{\text{in}}$ : 3.04 mm). The scattering parameters ( $S_{11}$ ,  $S_{21}$ ) were measured on the toroidal-shape composites by a network analyzer (Agilent Technologies

\* Corresponding authors.

E-mail addresses: [suzb33@ysu.edu.cn](mailto:suzb33@ysu.edu.cn) (Z. Su), [wenfsh03@126.com](mailto:wenfsh03@126.com) (F. Wen).

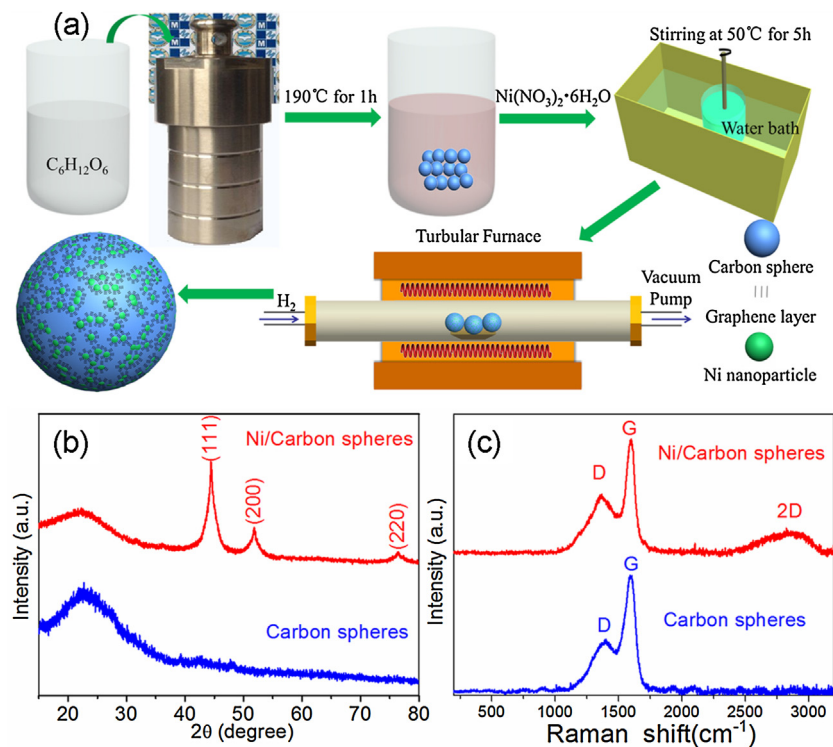


**Fig. 1.** Material synthesis processes for nickel nanoparticles incorporated carbon spheres (a); XRD pattern (b) and Raman spectra (c) of nickel nanoparticles incorporated carbon spheres.

E8363B) in the range of 0.1–18 GHz. The relative permeability ( $\mu_r$ ) and the relative permittivity ( $\epsilon_r$ ) were determined from the scattering parameters.

### 3. Results and discussion

Fig. 1(b) illustrates the XRD pattern of as-prepared carbon spheres and nickel nanoparticles incorporated carbon spheres. The XRD patterns of carbon spheres shows a broad peak, revealing amorphous state of carbon spheres, which is owing to a large number of amorphous carbon in the carbon spheres. The crystalline structure of the nickel nanoparticles incorporated carbon spheres was characterized by XRD, and according to the Scherrer formula, the average crystal size of nickel nanoparticles is deduced to be about 6 nm exhibiting a crystalline phase that can well indexed as cubic nickel phase with face-centered cubic (fcc) structure. The diffraction peaks at  $44.44^\circ$ ,  $51.83^\circ$  and  $76.42^\circ$  correspond to the respective (1 1 1), (2 0 0) and (2 2 2) planes of the nickel crystal lattice. The Raman spectra at room temperature of as-prepared carbon spheres and nickel nanoparticles incorporated carbon spheres is shown in Fig. 1(c). The Raman spectra of all samples exhibit two main broad peaks at  $\sim 1355\text{ cm}^{-1}$  marked as D peak for “disordered” and  $\sim 1590\text{ cm}^{-1}$  marked as G peak for “graphite carbon” [18]. No obvious change of the G/D ratio have been found which indicates the graphitic structure versus the degree of structural disorder and defects. The existence of the 2D at  $\sim 2815\text{ cm}^{-1}$  band confirms that nickel nanoparticles incorporated carbon spheres are graphitized. The broadening of the 2D peak can be attributed to the relatively small graphitic domain sizes or the large portion of edge atoms [19–21].

Fig. 2(a) and (b) shows the SEM images of carbon spheres and nickel nanoparticles incorporated carbon spheres. Carbon spheres with a diameter between 200 and 400 nm can be clearly observed, moreover aggregates of small nanoparticles can be observed on the surface of nickel nanoparticles incorporated carbon spheres.

Fig. 2(c) presents the TEM image of nickel nanoparticles incorporated carbon spheres. It can be observed that Ni nanoparticles with sizes of about 6 nm are well dispersed on the surface of carbon spheres which agree with the average crystal size obtained from the X-ray diffraction patterns. Fig. 2(d) shows the HRTEM of nickel nanoparticles incorporated carbon spheres. It clearly exhibits the signature image of the few-layer graphene. The measured lattice space of graphene layer is about 0.34 nm, which is in good agreement with the thickness of mono-layer graphene [22].

Fig. 3(a) shows the frequency dependence of the real part ( $\epsilon_r'$ ) and imaginary part ( $\epsilon_r''$ ) of relative complex permittivity of the nickel nanoparticles incorporated carbon spheres composites with 40 wt.%. The real part of relative complex permittivity  $\epsilon_r'$  declines from 3.2 to 2.6, moreover, the value of  $\epsilon_r''$  almost remain constant. Fig. 3(b) shows the frequency dependence of the real part ( $\mu_r'$ ) and imaginary part ( $\mu_r''$ ) of relative complex permeability of the nickel nanoparticles incorporated carbon spheres composites with 40 wt.%. The real part of relative complex permeability  $\mu_r'$  declines from 1.3 to 1.0, and the imaginary part  $\mu_r''$  declines from 3.8 to 0.04 with increasing frequency. Fig. 3(c) shows frequency dependence of the loss tangent of dielectric  $\tan\delta_E = \epsilon_r''/\epsilon_r'$  and magnetic  $\tan\delta_M = \mu_r''/\mu_r'$  of composites. It is obvious that magnetic loss is larger than dielectric loss from 0.1 GHz to 15.5 GHz, and magnetic loss is less than dielectric loss from 15.5 GHz to 18.0 GHz.

The frequency dependence of reflection loss (RL) values was estimated from the complex permittivity ( $\epsilon_r = \epsilon_r' - j\epsilon_r''$ ) and the complex permeability ( $\mu_r = \mu_r' - j\mu_r''$ ) refer to the following formulas [23–26]:

$$Z_{in} = Z_0 \left( \frac{\mu_r}{\epsilon_r} \right)^{1/2} \tanh \left\{ j \left( \frac{2\pi f d}{c} \right) (\mu_r \epsilon_r)^{1/2} \right\} \quad (1)$$

Download English Version:

<https://daneshyari.com/en/article/1486909>

Download Persian Version:

<https://daneshyari.com/article/1486909>

[Daneshyari.com](https://daneshyari.com)